Jordanian Journal of Computers and Information Technology (JJCIT), Vol. 12, No. 01, March 2026.

LOG-STAT: AN ILLUMINATION-BALANCING ALGORITHM FOR ARCHAEOLOGICAL IMAGES CAPTURED IN NON-IDEAL LIGHTING

Zohair Al-Ameen[1] and Basim Mahmood[2]

(Received: 18-Oct.-2025, Revised: 6-Dec.-2025, Accepted: 23-Dec.-2025)

ABSTRACT

Archaeological images are occasionally captured in environments with non-ideal lighting. This results in imbalanced illumination and a loss of detail. These problems hinder precise operations, such as analysis, interpretation, representation, and 3D modeling. This study introduces a non-complex illumination balancing algorithm called Log-Stat, leveraging logarithmic approaches and statistical methods. It also includes two main phases, one for illumination balancing and the other for tonality adjustment. The first phase utilizes six mathematical equations, while the second phase utilizes four equations, processing the V channel of the image in the HSV color model. Various images have been used to test the algorithm, and a comparison with ten prominent algorithms is achieved, evaluating the outcomes using six measures. The results have shown the success of Log-Stat in different aspects, including fidelity recovery and illumination balance. This allowed better visualization of details, which the unbalanced illumination effect hindered. Integrating appropriate methods and fine-tuning the parameters enabled the Log-Stat to perform in dissimilar illumination situations.

KEYWORDS

Archeology, Image enhancement, Log-Stat, Illumination balancing, Non-ideal lighting.

1. INTRODUCTION

Digital images are an essential tool in archaeology. They can be utilized for documenting, modeling, or recording findings [1]. However, their quality is often compromised, as various degradations may be included. One degradation of interest is the inconsistent illumination. It makes the image appear underlit (too dark) in certain regions, while appearing overlit (too bright) in the other areas [2]. This yields an undesirable appearance and loss of central details, such as textures, affecting the overall visibility [3]. Other image aspects, such as colors, are also affected due to uneven illumination. Colors appear mispresented, leading to struggles in distinguishing and perceiving the actual information precisely [4]. Overall, inconsistent illumination influences the accurate analysis, extraction, and representation of archaeological subjects. As imaging technology advances, the ability to enhance images has become considerable in archaeological research [5]. Digital images enable non-invasive inspection of scenes. This avoids further deterioration and protects integrity. Thus, high-quality images become a key element [6]. This study addresses the illumination balancing issue by exploring logarithmic and statistical methods to improve accuracy and visibility. The lighting situations in archaeological settings are usually far from ideal. This is due to various factors. Natural light can be limited or insufficient, especially in indoor settings. The nature of the photographed object can also affect the lighting conditions. Reflective or shiny surfaces cause glare, whereas textured surfaces cause shadows [7]. Likewise, artificial lighting, such as flashlights, can lead to inconsistent illumination [8].

Uneven illumination poses significant challenges to archaeologists, distorting the colors and obscuring the details [9]. Without adequate balance, the accuracy of image-based analysis is compromised. Restoring images must be carried out effectively to obtain improved-quality images without generating processing errors [10]. Hence, the key contribution of this research is to develop a non-complex algorithm that rapidly and adequately balances the illumination of archaeological images while avoiding limitations, such as shadows around edges, brightness amplification (i.e., global increase in brightness), over-enhancements, and distortions. In this context, balancing the illumination offers the following benefits: (i) it improves clarity and visibility, leading to more reliable interpretations; (ii) it helps reduce

1. Z. Al-Ameen is with the ICT Research Unit, Computer Center, University of Mosul Presidency, University of Mosul, Mosul, Nineveh, Iraq. Email: qizohair@uomosul.edu.iq
2. B. Mahmood is with the Computer Science Department, College of Computer Science and Mathematics, University of Mosul, Mosul, Nineveh, Iraq. Email: bmahmood@uomosul.edu.iq

distortions caused by glare, shadows, and over- or under-exposure, leading to a more realistic appearance. Thus, the Log-Stat algorithm is developed, combining logarithmic and statistical processes for satisfactory illumination balancing. The development aligns with ongoing efforts to create better methods for the digitalization of cultural heritage. The novelty of Log-Stat lies in its two-stage design, which jointly addresses illumination balancing and tonality adjustment in an integrated framework. The first phase redistributes intensity using logarithmic-based approaches infused with statistical measures to brighten under-lit areas and balance the overall illumination. The phase stage adjusts the tonality using tailored statistical methods. The unique combination of mathematical equations in both phases has not been reported in existing algorithms.

When developing Log-Stat, the key objective was to create an expeditious illumination balancing algorithm that can handle different lighting scenarios. Moreover, it is explicitly designed to preserve the structural integrity and tonal consistency of vital archeological features. By leveraging logarithmic and statistical approaches, an integrated framework has been created that mitigates excessive darkness or brightness. This ensures nuanced features and material variations remain visually distinguishable. The design also incorporates color preservation, implemented only on the value channel of the Hue, Saturation, and Value (HSV) color space. This prevented color shifts and preserved saturation fidelity that can misrepresent the intended appearance of the scene. As a result, Log-Stat is principally suitable for the archaeological domain, where precise visualization of details is vital. The intended target audience includes researchers and experts who require an unfailing enhancement method that improves the perceptibility and interpretability of images without compromising the visual accuracy of the content. Intensive tests are conducted, and the vital findings are reported. This study incorporates tailored image processing procedures, enabling the acquisition of more information from captured images using practical solutions. Ultimately, the findings of this research will have a lasting impact on archaeology, benefiting both current and future researchers. This paper is organized as follows: Section 2 reviews the related work; Section 3 describes the proposed algorithm; Section 4 provides the results, comparisons, and required analysis; Section 5 delivers the key conclusions.

2. RELATED WORK

In past years, this topic has been of interest to many researchers, who have developed and introduced various concepts. In 2015, a probabilistic model (PM) was proposed [11], which utilizes PM as a maximum *a posteriori* (MAP) to approximate the illumination and reflectance of the input image in the linear domain. Then, logarithmic transformations are implemented to determine which transformation provides better performance. Accordingly, the MAP model is converted into an energy-minimization domain, and an alternating direction of multiplier model is implemented. In 2016, a fusion-based method (FbM) was introduced [12], which runs a morphological closing process to estimate the illumination part. Next, two versions of the illumination part are produced, representing contrast-enhanced and illumination-enhanced counterparts using the contrast-limited adaptive histogram equalization (CLAHE) method and a sigmoid function. A customized weight is designed for each version, and a multi-scale fusion model is implemented to create an adjusted-illumination part. Lastly, the output image is created by reimbursing the adjusted-illumination part with the reflectance part. In 2017, an algorithm named LIME was presented [13], in which the illumination part is estimated by finding the maximum RGB value for each pixel. The illumination part is refined by using a structure prior model to create the final illumination part. Finally, the refined illumination is used with the reflectance to output the image.

In 2018, another algorithm, called LECARM [14], was offered, which utilizes the response characteristics of cameras. Initially, a proper response model and its variables are set. After that, the illumination part is estimated *via* an exposure-ratio model for every intensity. Using an approximation ratio map, the selected response model is then used to modify every intensity value to a satisfactory exposure. In 2019, a gradient-based method (GbM) was developed [15], focusing on improving the gradients in the dark areas, as they are more sensitive to human vision. In this algorithm, the gradients of the input image are first extracted to be enhanced using a customized method. Next, optional gradient filtering is applied, followed by an image-integration process that utilizes intensity-range constraints to preserve the gradient components while increasing the intensity to a certain amount. In 2020, a semantic-guided method was delivered [16], focusing on harnessing image semantics. The semantic segmentation approach initially obtains the image areas with designated semantics. Next, the semantics are combined and refined with an illumination map estimated from the illumination part. Next, the dark areas are

enhanced by guiding the semantic information.

In 2021, a reflection model (RM) was introduced for illumination balancing [17], *via* the aid of the principal-component analysis (PCA) notion. It first stretches the dynamic range of the color image to correct the contrast, then converts the image into the HSV color model. The V component is processed using the multi-scale theory to get the illumination part. Next, the Fechner model is applied to improve the illumination. After that, a PCA-based fusion process is applied to combine the two images. Then, the contrast is enhanced using the CLAHE method. Finally, a transformation back to the RGB color model is attained to create the output image. In 2022, an atmospheric light-based method was proposed [18], keeping it simple by not requiring training or refinement. This method connects the atmospheric scattering and retinex models to adjust the illumination. Moreover, the medium transmission is computed from the saturation information, and the adaptive saturation of scene radiance is approximated using a non-complex approach. In 2023, a sharpening-smoothing method (ShSm) was developed [19], which processes the *V* channel only after converting from RGB into HSV. After that, a multi-scale decomposition process is applied to estimate the details of the sub-images. Next, the CLAHE method is applied to the last estimation for contrast enhancement. Moreover, the details of the sub-images are improved and added to the contrast-enhanced ones. Finally, an RGB image is created by applying the inverse HSV transform, representing the final image.

In the same year, another concept was presented for illumination balancing; namely, the triangle similarity model (TSM) [20]. It works in the HSI domain, specifically the *S* and *I* channels. It implements scaling and translation processes to improve saturation and intensity, while preserving the H component from modifications. It also implements five model-based enhancement procedures to produce images with better-balanced illumination. In 2024, a generative adversarial network was introduced [21], comprising two main networks: the generative network and the adversarial network. The first includes dilated and regular convolutions with max and average pooling, acting as a multi-scale feature extractor to get better feature information. In addition to these two networks, an illumination attention model is employed to reduce feature redundancy by assigning higher weights to significant features. An upgraded loss function is added to decrease color distortions in this context. Many of the reviewed methods utilize CLAHE as an enhancement module. It works by splitting a given image into small, non-overlapping tiles, then applying histogram equalization to each tile to reallocate its pixel intensities. Next, each tile's histogram is clipped using a predefined clip limit, and the surplus pixels are reallocated evenly across all histogram bins to prevent intensity over-amplification and suppress noise. Finally, a soft-interpolation process is applied between neighboring tiles to avoid block artifacts [22].

In recent years, attention has turned to the development of learning [23], coarse-to-fine [24], or AI-based [25] algorithms. One of the branded learning-based frameworks in this area is the LightenNet, which was presented in 2018 [26]. It is a convolutional neural network (CNN)-based method that adopts a retinex-inspired design. In this method, the network learns to approximate the illumination rather than performing direct processing. This approach enables better illumination balancing with minimized artifact generation. Another neural-network framework named CIE-XYZ Net was introduced in 2022 [27]. It is designed to map images back to a more meaningful representation, operating under consistent assumptions of color and illumination. This approach bridges the gap between publicly available processed images and raw ones. In 2023, a method named Retinexformer was introduced [28]. It is a deep learning-based algorithm that utilizes a one-step Retinex framework (OSRF) instead of multi-step frameworks. OSRF initially approximates the illumination components to enhance the dimmed regions and restore the corrupted parts, delivering the output image. This includes the utilization of an illumination-guided transformer (IGT) that employs illumination information to guide the modeling of non-local connections found in non-uniformly-lit regions. Simply put, Retinexformer is obtained by plugging IGT into OSRF.

In 2024, ConvIR was introduced [29], a lightweight CNN-based algorithm for image restoration. It relies on the CNN architecture to learn end-to-end mapping from degraded sets to clean targets using a convolution feature-extraction scheme. Despite its simplicity, it achieved competitive performances. Still, its effectiveness is based on the alignment between real-world scenarios and training data. In 2025, UPT-Flow, a multi-scale transformer, was presented [30]. This method utilizes a learning transformer backbone to model intricate allocations of intensities, allowing controlled mapping to generate illumination-corrected results. Unlike conventional learning-based approaches, this method uses a probabilistic-learning framework that preserves structural information when adjusting for illumination.

As observed from the reviewed methods, various concepts have been developed, ranging from simple to complex, standard to AI-based. Despite significant advances in this field, not all the introduced algorithms are perfect, as some introduce artifacts, such as halos and distortions, others are of high complexity, and others are inapplicable for real-life applications. Thus, existing algorithms still struggle under non-ideal lighting conditions. Classical algorithms, such as Retinex or histogram equalization, cannot be used, as they provide blind global processing without considering the spatial context and delicate details.

Their improved counterparts mitigated these issues, but are still struggling in this context, as artifacts may still be introduced along with deficient processing abilities in different scenarios. Moreover, despite the increased use of deep-learning and AI-based methods in recent years, image-processing algorithms remain critical for archeological images due to their computational efficiency, reproducibility, and interpretability. In this context, datasets are often limited, making deep-learning methods less practical, as such methods require extensive training. Besides, they act as a black-box, limiting their reproducibility. Moreover, image-processing methods are preferred in domains such as archeology, because they are mathematically transparent, methodical, and reproducible, ensuring long-term reliability and interpretability. Thus, the door remains open to develop an algorithm that considers the advantages and avoids the disadvantages of the reviewed methods, tailored to the nature of the archaeological images. The developed Log-Stat addressed these issues by utilizing a dual-phase approach for illumination balancing and tonality adjustment, operating in a fully transparent and parameterizable manner. This allowed experts to comprehend and control the processing procedure, thereby enabling interpretability, reproducibility, and tracability. Compared to classical, improved, and deep-learning methods, Log-Stat delivers a principled, transparent, fully explainable solution customized to the subtle challenges of archaeological lighting conditions.

3. PROPOSED ALGORITHM

Balancing uneven illumination after image capturing is uneasy and requires customized algorithms to achieve this task successfully. Hence, a tailored algorithm named Log-Stat is developed to balance the inconstant illumination. The name "Log-Stat" signifies two main aspects: logarithmic operations (Log) and statistical methods (Stat). This means that the proposed algorithm relies heavily on these aspects to balance the illumination of a given image. The Log-Stat algorithm starts by changing the input image to the HSV model and processing only the value channel V (being in a 0 to 1 range) while not modifying the other channels. All the equations receive images with a zero-to-one range, avoiding issues, such as under- or overflow during calculations. This aligns well with floating-point arithmetic, which is a prevalent practice in modern processing frameworks. Although the HSV is a non-perceptual color model, it is preferred over color models, such as CIELAB, because it provides a more direct way to enhance the illumination without affecting the colors. In HSV, the V channel corresponds directly to intensity, while in CIELAB, for example, improving the luminance channel L can alter the chromatic components and unintentionally affect the colors. Moreover, HSV is computationally more effective, making it a desirable choice for many real-life applications. The algorithm receives channel V and parameter γ, a numerical value responsible for the illumination level, such that $\gamma > 1$, and a higher value leads to less illumination and further adjusted tonality. Channel V is first processed using Eq. (1) [31]:

$$I_1 = \log\left(V + \varepsilon 1\right) \tag{1}$$

where I_1 is the resulting channel, and $\varepsilon 1 = 0.001$ is a small value to avoid the log of zero, which is infinity. The log transform expands the intensity range to improve visual details in dark regions while compressing the intensity range in brighter areas. This makes it particularly useful for balancing uneven illumination phenomena. Accordingly, a single log transform may help with illumination balancing. Still, it is frequently insufficient individually, especially for archaeological images where lighting situations vary substantially, as it applies a unified effect for all intensity values, which is not ideal for uneven lighting. Thus, a different log transformation is used for bright and dark areas to achieve a more balanced enhancement. Different transformers were found when searching for another log transformation that can contribute to providing better adjustments. One transform of interest is the transform given in [32], which is simple and better compresses higher values while expanding lower values. The second transformer is expressed in the following manner:

$$I = \frac{\max(V)}{\log(\max(V)+1)} \cdot \log(V+1) \tag{2}$$

where · is a multiplication operator, and *max* denotes the highest value in the array. The log transformation in Eq. (2) must be adapted to the nature of the research problem to perform a better job of illumination balancing. Hence, this transformer was heuristically modified to become:

$$I_2 = \frac{-\sigma(V)}{\log(\sigma(V)+1)} \cdot \log((0.925-V)+\varepsilon 2) \tag{3}$$

where σ represents the standard deviation of V and $\varepsilon 2 = 0.09$. This transformer achieves the following points. First, it provides better compression for high values and boosts low values, making details in shadows more noticeable. Second, it reverses the intensities, changing white to black and black to white, acting as a map, where the dark spots exist and are converted into white for addition in the next step, thereby achieving better illumination balancing. The standard deviation is used, as it adapts based on the image tonality, meaning that the effect changes depending on the statistical properties of each input image. Figure 1 provides an intuitive visual demonstration of why to use Eq. (3) instead of Eq. (2) in Log-Stat.

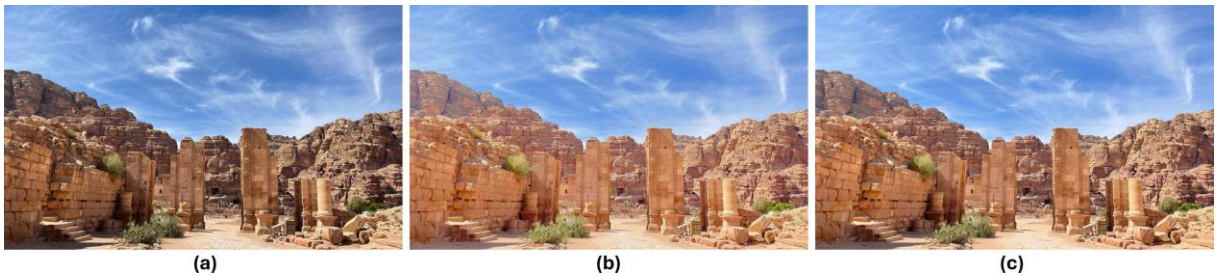

Figure 1. Intuitive visual demonstration of utilizing Eq. (3): (a) Under-lit image; (b) Using Eq. (3) with Log-Stat; (c) Using Eq. (2) with Log-Stat.

Next, the outputs of Eq. (1) and Eq. (3) are combined using a logarithmic image-processing (LIP) addition model. The LIP addition models combine two images to provide a more meaningful output image. Different models exist in this context, and one model of interest is the one introduced by Jourlin and Pinoli [33], which can be expressed as:

$$\boldsymbol{L = (I_1 + I_2) + (I_1 \cdot I_2)} \tag{4}$$

As simple as it may seem, it has drawbacks. The term ($I_1 \cdot I_2$) causes a noticeable increase in intensity values, especially the high-intensity ones, leading to over-brightening the bright areas. Thus, this term is replaced, and the equation is modified to become:

$$\boldsymbol{I_3 = (I_1 + I_2) \cdot (1 - I_1)^{0.1}} \tag{5}$$

In this context, this model performs a non-linear addition process, enhancing darker areas more effectively. The term $(1\text{-}I_1)^{0.1}$ compresses high-intensity values, ensuring that brightness does not unnecessarily increase, which occurs in standard LIP models. The LIP model in Eq. (5) improves the illumination in the dark regions without extremely brightening the bright areas. Figure 2 demonstrates the sensitivity analysis for Eq. (5).

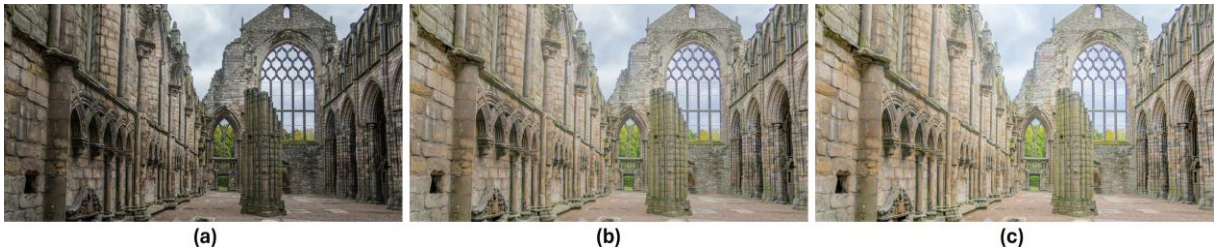

Figure 2. Sensitivity analysis for Eq. (5): (a) Under-lit image; (b) Exponent = 0.1; (c) Exponent = 1.

As observed in Figure 2, the use of exponent = 0.1 in Eq. (5) helped deliver natural overall illumination z and did not increase brightness, especially in the cloud area in the sky. However, when employing exponent = 1, the overall illumination showed a slight increase. Moreover, the brightness in the cloud area was also increased, which is undesirable. Next, three more models are utilized to balance illumination, which are the following ones:

$$I_4 = 1 - \left(\frac{I_3 - \min(I_3)}{\max(I_3) - \min(I_3)} \right) \tag{6}$$

$$I_5 = 1 - (I_4 - I_1) \tag{7}$$

$$I_6 = \frac{I_5 - \min(I_5)}{\max(I_5) - \min(I_5)} \tag{8}$$

Eq. (6) performs statistical normalization [34] and inversion. Normalization redistributes I_3 values to the full range of zero to one, ensuring that the image intensities fall within the proper image range. Subtraction from one makes dark areas bright, and *vice versa*, reversing the action of inversion performed in Eq. (3). As for Eq. (7), it alters I_4 by subtracting I_1 to ensure the primary illumination structure is maintained, harmonizing the illumination-balancing process, so that the output does not drift too far from the input, and ensuring that the balancing effect is not over-darkened or over-brightened to provide better naturality. In addition, this step is not purely subtractive, but it reconstructs a compensated-illumination image by reintegrating structural information derived from I_3. Eq. (8) rescales the intensities of I_5 to a valid image range [34]. At this point, the illumination is balanced, illuminating the dark regions while maintaining bright regions from being over-illuminated. Still, the totality of the output image I_6 is not well-adjusted, and it appears to have foggy and washed-out effects. Thus, a tonality-enhancement model is applied to I_6, which includes four distinct steps, expressed as:

$$T_1 = 1 - \exp\left(-\frac{I_6}{\sqrt{I_6}} \right) \tag{9}$$

$$T_2 = \frac{1}{1 + \left(\frac{I_6}{\gamma} \right)^{-\gamma}} \tag{10}$$

$$T_3 = \left(T_1 + (T_1 \cdot T_2) \right)^{\gamma} \tag{11}$$

$$T_4 = \frac{T_3 - \min(T_3)}{\max(T_3) - \min(T_3)} \tag{12}$$

Eq. (9) is a modified Rayleigh cumulative distribution function (MRCDF) [35], a statistical method that acts as a curvy transformation and can enhance the tonality by non-linearly mapping the intensities. It modifies the dynamic range by increasing lower values, but relatively unchanging higher ones. Eq. (10) is the gamma-adjusted CDF of the log-logistic distribution (GA-CDF-LLD) [36], a modified statistical method used to improve mid-tones while preserving very bright and very dark regions, with the help of the γ parameter, in that higher values boost mid-tones. Eq. (11) is the modified LIP model given in Eq. (4), which combines the output of Eq. (9) and that of Eq. (10), since a single mathematical method cannot achieve the task of tonality enhancement. This equation performs an overall-tonality refinement based on the value of the γ parameter, providing an adaptive increase in the difference between the lowest and the highest intensities, attenuating the foggy effect. The T_2 term is missing from the additive part in Eq. (11), because when adding it, it slightly dims the overall brightness. That's why it is removed to allow better overall-illumination representation and to reduce computations. Eq. (12) is the final equation, which is the statistical normalization [34] applied to ensure that no intensities fall outside the display range, preventing loss of dynamic range and improving the overall tonality of the output. The output of Eq. (12) is the enhanced value channel. Thus, a conversion into the RGB color model is applied, generating the output image.

Regarding the coupling role in Eqs. (10) and (11), an ablation study has been conducted to prove the effectiveness of coupling. Accordingly, γ was used only for Eq. (10), while fixing it for Eq. (11). The results in Figure 3 reveal that decoupling led to inconsistent and unstable behavior with different γ

values. Hence, low values (γ=1-3) under-enhanced the image and were unsuccessful in recovering acceptable visibility. Values over 7 (γ=10-100), on the other hand, did not affect the output; it's like that the algorithm lost its adjustment control. This instability arose, because these two equations jointly regulate the tonal adjustment. When they are decoupled, the two equations respond in conflicting ways, which makes it unpossible to uphold a balanced enhancement. In contrast, the coupling strategy allowed intrinsic synchronization between fusion strength and tonal adjustment. As a result, natural, stable, and visually coherent results are obtained when the coupling strategy is utilized. These findings rationalize the design choice of enabling the coupling role of γ to coordinate the two operations and verify that the coupling process is vital rather than arbitrary.

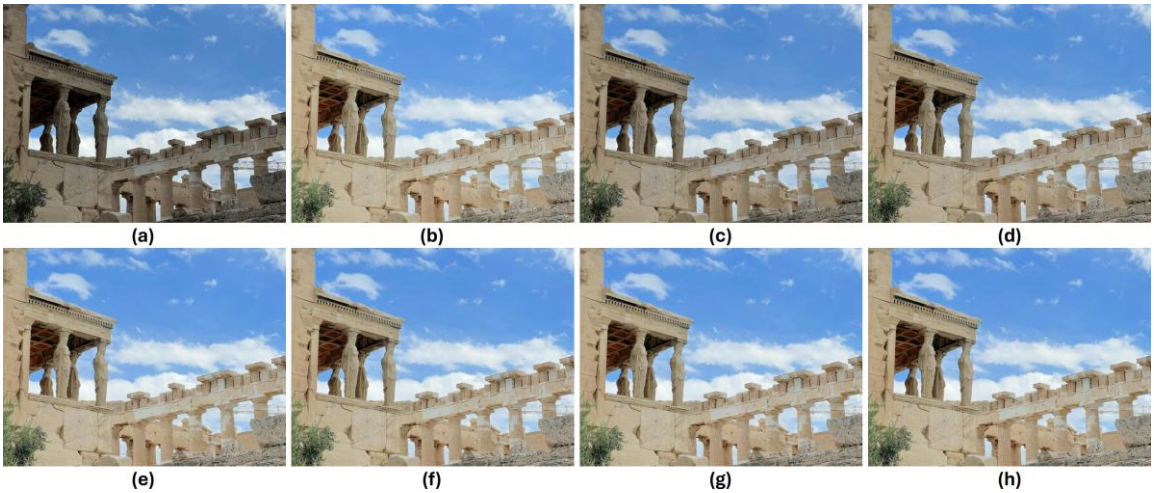

Figure 3. Ablation study (justifying the coupling effect): (a) Under-lit image; (b) Standard setting: coupling effect with γ = 7; Decoupling effect using fixing exponent for Eq. (11) at 7 and γ is equal to: (c) γ = 1; (d) γ = 3; (e) γ = 10; (f) γ = 20; (g) γ = 50; (h) γ = 100.

The diagram of the Log-Stat algorithm is given in Figure 4. In sensitive areas, such as archaeology, classical image-processing frameworks are often chosen, because their operations are transparent and methodically reproducible. They apply mathematically-defined approaches, permitting one to understand exactly how each step modifies the image. This clarity helps uphold subtle features without introducing artifacts or unrealistic details, which can occur in AI or deep learning-based methods. Classical frameworks also allow accurate parameter control, making it easier to adapt processing to uneven-illumination challenges, while ensuring that the outcomes remain true to the original scene. Thus, classical transformations have been utilized with Log-Stat to achieve these targets.

4. RESULTS AND ANALYSIS

This section explains different aspects related to the outcomes. The dataset was collected from https://unsplash.com/, one of the largest photo-stock websites online, containing millions of uncopyrighted images that can be used free of charge. A thorough search was conducted on this website, and 200 images were collected, representing a diverse range of archaeological scenes. In this paper, no dedicated pre-processing was carried out on the dataset images. This is deliberate, because the purpose is to evaluate the general applicability and reliability of Log-Stat when used with real-world archeological images without any form of enhancement. As for the image-selection procedure, it was conducted in a semi-random manner from the collected images. Moreover, this procedure is implemented without imposing restrictions on the image content or the severity of lighting. This tactic ensures that the assessment truly reflects natural and diverse occurring image-lighting conditions rather than a curated selection tailored to Log-Stat strengths. It is also worth noting that no unified dataset has been used, as the intention was to evaluate performance under challenging illumination conditions in real-world scenarios. Such conditions vary widely and cannot be fully signified by a standardized dataset. Thus, diverse real-world examples were employed intentionally to capture the variability and complexity of archaeological scenes. This allows a more meaningful assessment of Log-Stat's practical effectiveness. Also, it shows its ability to handle challenging illumination conditions posed by the scene environments.

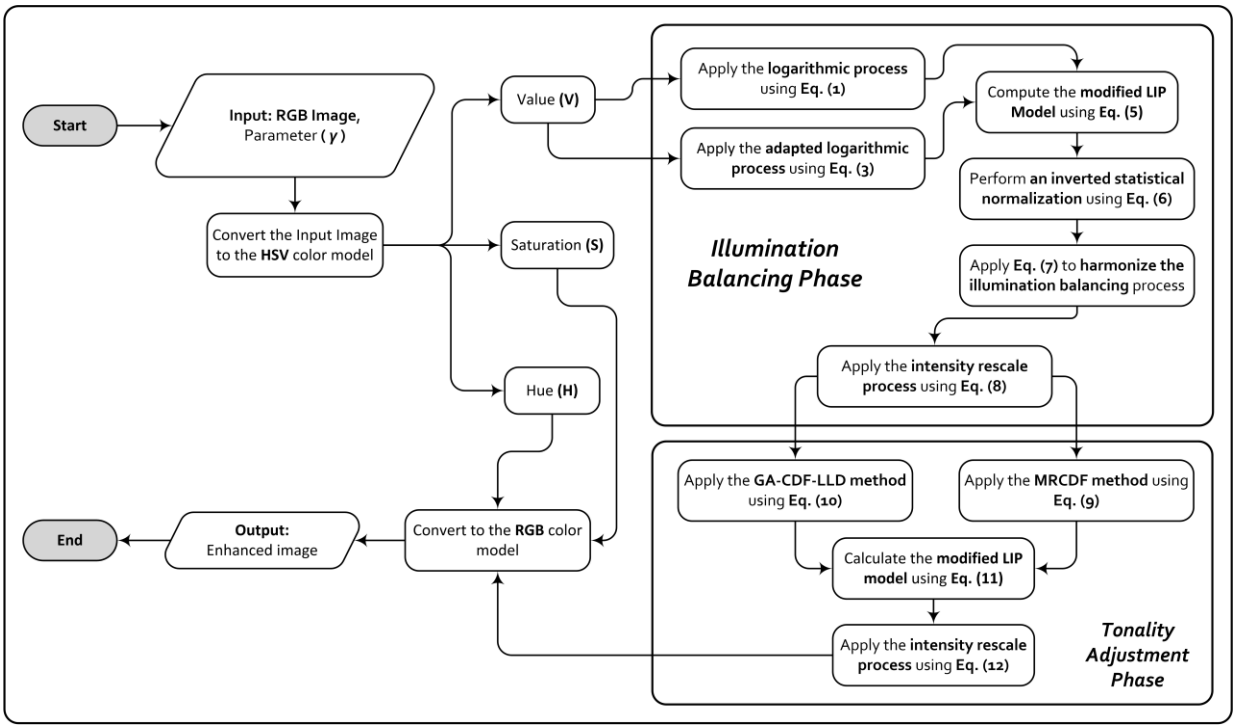

Figure 4. Illustrative diagram of the Log-Stat algorithm.

The experimental results are divided into three categories. The first category describes the effects of changing the value of γ. It is provided to offer a visual understanding of what γ does to the image when it changes, with sample results shown in Figure 5. The second category demonstrates the ability to process noisy images, and the outcomes are shown in Figure 6. The third category is processing various archaeology-related images and showing the before and after versions to demonstrate Log-Stat's capabilities. The results of this action are shown in Figures from 7 to 9. Besides, the proposed algorithm is compared with ten contemporary algorithms. The comparison methods are PM, FbM, LIME, LightenNet, LECARM, GbM, RM, ShSm, TSM, and Retinexformer, which are reviewed in the related work section. All experiments and comparisons are performed using a laptop equipped with an i5-1135G7 2.40 GHz processor and 16 GB of RAM. The comparison results are given in Figures from 10 to 13 and Tables from 1 to 6. The image sizes of Figures from 10 to 13 are: (6240×4160), (3200×1975), (4032×3024), and (4274×3205), respectively. In this context, an insightful analysis of the results of each category is given. Then, this section ends with key remarks. For performance measurement, six measures were used, which are: lightness order error (LOE) [37], blind multiple pseudo-reference index (BMPRI) [38], color-quality measure (CQM) [39], perception-based image-quality evaluator (PIQE) [40], gradient magnitude with Laplacian of Gaussian(GM-LOG) [41], and runtime (RT) [42].

LOE is a reduced-reference metric used for quantifying the relativity of lightness-order, meaning how much the brightness grade among neighboring pixels is preserved after enhancement. This reflects illumination's naturalness and perceptual consistency, in that if LOE is significantly changed, the enhanced image appears artificial or unnatural. BMPRI is a no-reference metric that measures naturalness and artifact presence, aiming to reflect how humans perceive the image. CQM is a no-reference metric that measures color quality using three perceptual attributes: contrast, colorfulness, and sharpness, aiming to mimic human perception of observing colors. PIQE is a no-reference metric that evaluates how a given image diverges from undistorted and natural visual features. It measures perceptual distortions. GM-LOG is also a no-reference metric that evaluates a given image based on the statistics of gradient information. It assumes that high-quality natural-looking images follow foreseeable gradient patterns, because they are highly structured, and degradations distort these patterns and deform the structure. It measures structural naturalness. RT is a measure used to quantify the computational cost of given algorithms, which is essential to assess their practical usability. Even if the algorithms are based on dissimilar concepts, RT delivers insight into computational efficiency and suitability for real-life or resource-limited applications. For LOE, PIQE, and RT, lower scores indicate better performances, meaning that the enhancement preserved more natural illumination relations for LOE, fewer perceptual

distortions for PIQE, and faster implementation for RT. In contrast, higher scores indicate better performances for BMPRI, CQM, and GM-LOG, suggesting more perceptual details, higher color quality, and better structural naturalness.

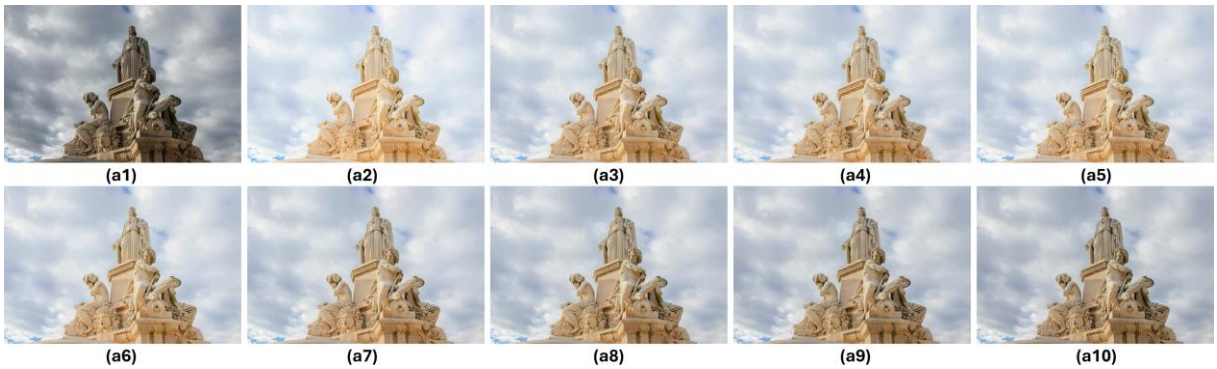

Figure 5. The impact of changing γ. (a1) unevenly-illuminated image. Log-Stat processed other images with γ equal to: (a2) 1; (a3) 2; (a4) 3; (a5) 4; (a6) 5; (a7) 6; (a8) 7; (a9) 8; (a10) 9.

The results in Figure 5 illustrate the effect of changing γ, where the brightness decreases when γ increases in value, and the tonality further improves. This indicates that there is an inverse relation between brightness and γ, while the relationship is direct when it comes to tonality. Moreover, it is observed that the visibility of the details, specifically in the highlights and shadows, is enhanced with mediocre γ values. The image appears overly illuminated around (a2) to (a3), which may lead to the loss of certain fine details and an unnatural appearance. In addition, as γ increases, the image progressively darkens, balancing the illumination and enhancing the tonality. It is noticed that a moderate γ value (around 4-7) appears to provide a well-balanced illumination without over-exposure. Thus, the choice of γ is image-dependent based on specific features and the required illumination boost level. In this field, it is often preferred to use a manual enhancement parameter rather than an automatic one, as such images present unique and highly variable challenges that automation may not address effectively. Shadows, uneven lighting, and irregularities can confuse automated algorithms, leading to over- or under-correction. In contrast, manual adjustment enabled fine-tuning, allowing higher accuracy and improved extraction of meaningful information. Figure 6 shows the performance of Log-Stat when applied to noisy images. The original images shown in (a1, b1) exhibit noticeable illumination non-uniformity, with their zoomed-in views (a2, b2) revealing pronounced noise and texture degradation. After processing with Log-Stat at two γ settings (6 and 10), the resulting outputs (a3, b3, a4, b4) show notable improvement in tonality and illumination balance.

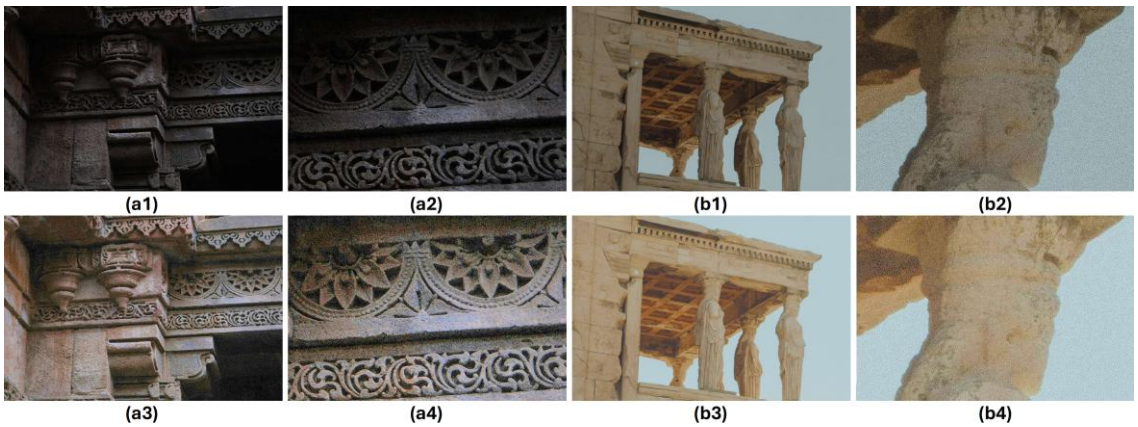

Figure 6. Log-Stat results with noisy images. (a1, b1) unevenly-illuminated images. (a2, b2) zoomed-in regions of (a1, b1) images. (a3, b3, a4, b4) processed by Log-Stat with γ = 6 and 10.

While some noise became more visible, especially in darker and shadowed regions, the structural details and textures have been improved. This indicates that the algorithm upholds its enhancement capability under noise conditions, though higher γ values may reveal more noise. Despite this, the algorithm does not introduce edge artifacts or artifacts, keeping the enhancement process structurally reliable even in

noisy conditions. Moreover, despite mild noise revelation with higher γ in some images, this behavior is anticipated and does not undermine the purpose of Log-Stat. This is due to it being designed exclusively for illumination balancing, not for denoising. Thus, it processes under the principle of maintaining the pristine image features while balancing illumination. Accordingly, when the brightness is increased in the dark regions, the formerly hidden noise logically becomes more visible. This does not mean that Log-Stat introduces or increases noise, but means that it uncovers existing noise that was concealed by low brightness. This result is consistent with most illumination-balancing algorithms that do not utilize a specialized denoising model. More importantly, the goal of Log-Stat is to achieve consistent, natural, and accurate illumination balancing without amplifying existing noise or introducing artifacts, which is attained successfully. Integrating a denoising model would risk altering image details, which is not desirable for archaeological images.

From the experimental results in Figures from 7 to 9, an overall improvement in quality is observed, as the processed images have balanced illumination and improved tonality compared to the original versions. Moreover, the shadows in certain areas are attenuated, making details in the dark regions more visible. Likewise, the fine surface textures appear more distinct and clearer. For example, in the images containing carvings in Figures 9e1 and 9e2, the sophisticated features of the sculptures are more pronounced after filtering. As for colors, the filtered images preserve natural color tones while handling the undue bright or dark regions, and the Log-Stat does not introduce color distortions.

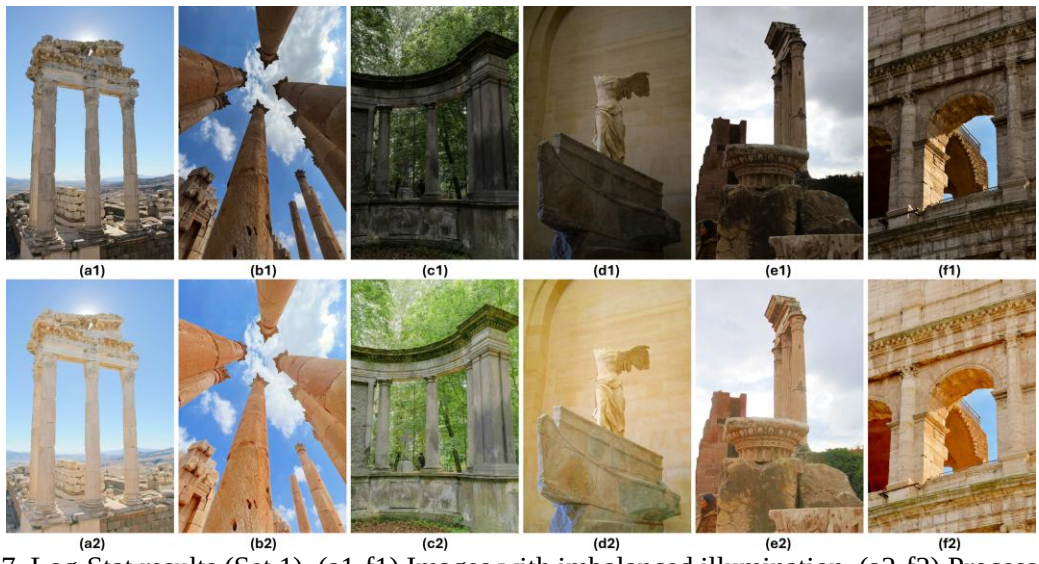

Figure 7. Log-Stat results (Set 1). (a1-f1) Images with imbalanced illumination. (a2-f2) Processed with γ = (3.5, 4, 6, 5, 5, and 4.5).

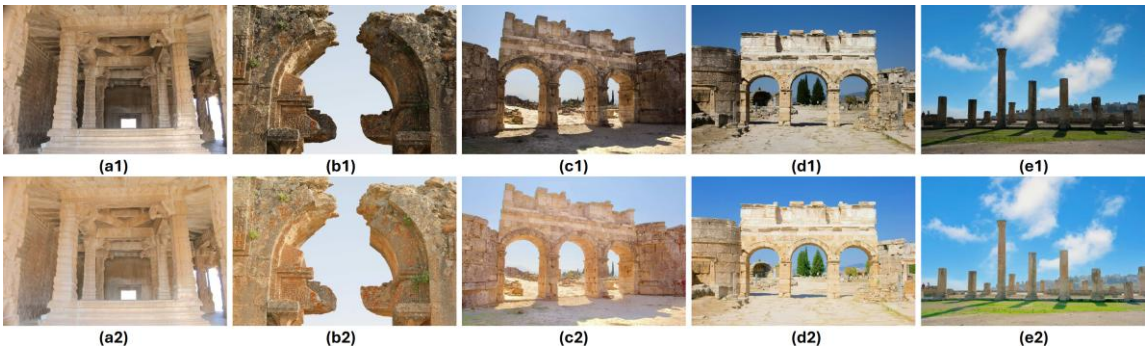

Figure 8. Log-Stat results (Set 2). (a1-e1) Images with imbalanced illumination. (a2-e2) Processed with γ = (3, 3.5, 6, 6, and 6.5).

As for shadows, original images contain sturdy shadows due to inconsistent lighting conditions. Still, Log-Stat has weakened such effects, delivering a pleasing appearance across the structures. This indicates that it effectively corrects these under-exposed areas, making formerly dark areas more evident. For example, the inner parts of the temple in Figures 8a1 and 8a2, which were dark, are now brighter and display more visible structural details. In Figures 8c1 and 8c2, the rock archway had a

darkened foreground. Now, the structure appears uniformly bright. As for illumination, it seems natural and avoids unnecessary over-exposure, ensuring that details are retained while upholding balance between tonality and texture. Likewise, a better color balance is observed, especially with warm tones (sandy and brown). Other colors, such as the blue in the sky, appeared more vibrant without looking unnatural. Moreover, it did not introduce major color distortions. Such enhancements have improved the overall scene clarity, achieving the key objective of the algorithm.

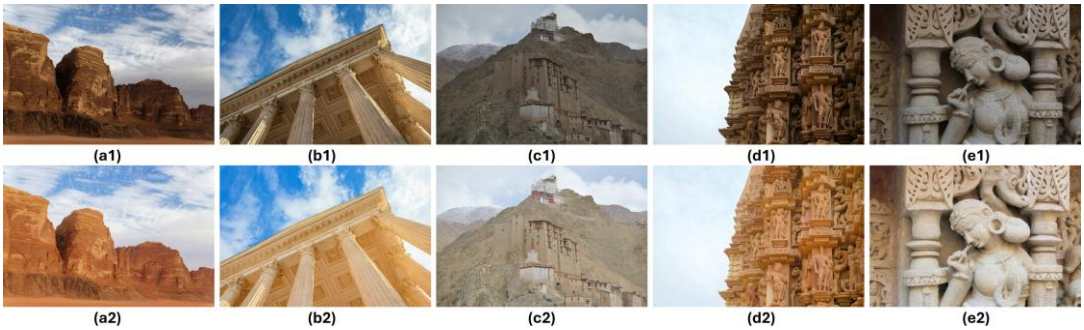

Figure 9. Log-Stat results (Set 3). (a1-e1) Images with imbalanced illumination. (a2-e2) Processed with γ = (6, 5, 1.5, 6, and 5.5).

Although certain processed images may appear visually similar to over-exposure, this is an unintended brightness increase, but in fact, it is the effect of illumination balancing. The intended illumination-balancing process should brighten shadowed areas and adjust the illumination across the scene. This makes previously obscured surfaces appear brighter and more uniformly illuminated. The illumination balancing may give certain regions a washed-out appearance when compared to their dimmed counterparts, but in fact, this is the balancing result that makes certain surfaces appear brighter, even though intensities remain within a valid range with no saturation occurrence. This also reflects Log-Stats's emphasis on revealing hidden details rather than preserving pristine non-uniform lighting. To be more specific, the textural information is not lost or degraded. However, it becomes more uniformly lit once shadows are attenuated and under-illuminated areas are brightened.

The comparison results are shown in Figures from 10 to 13. Tables from 1 to 6 demonstrate the dissimilarity of each algorithm in illumination balancing. All have improved the illumination, each in its way. The measures used indicate the following: LOE (illumination naturalness), RT (execution speed), BMPRI (perceptual clarity), CQM (color quality), PIQE (perceptual distortions), and GM-LOG (structural naturalness).

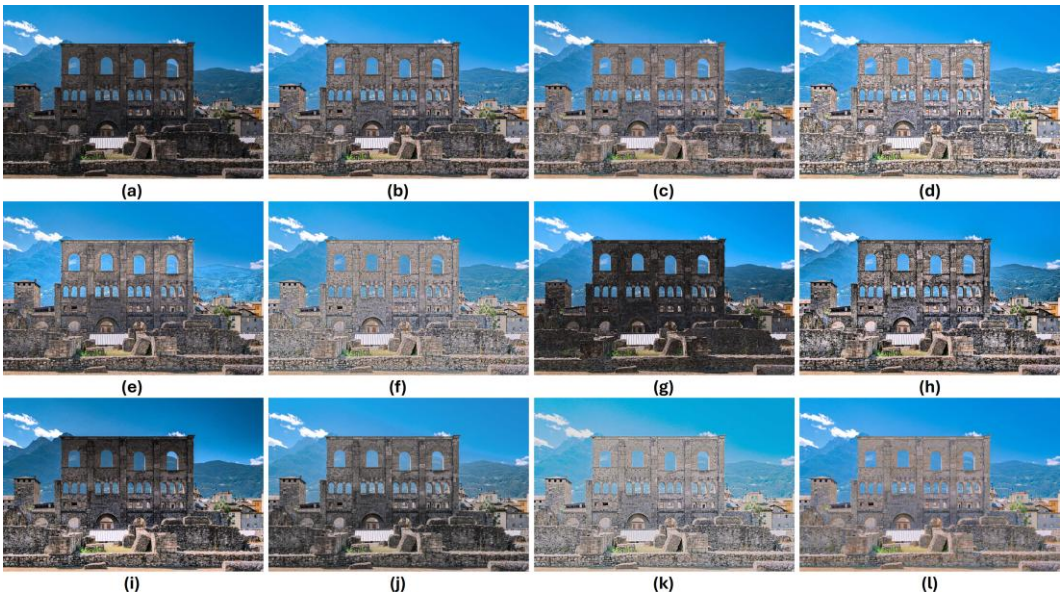

Figure 10. Results of comparisons (Batch 1): (a) Original image; images (b-l) are processed by: (b) PM; (c) FbM; (d) LIME; (e) LightenNet; (f) LECARM; (g) GbM; (h) RM; (i) ShSm; (j) TSM; (k) Retinexformer; (l) Log-Stat.

The performance ranking is set from worst to best as follows: lowest, below-low, low, above-low, below-mediocre, mediocre, above-mediocre, below-high, high, above-high, and best. The analysis is based on these attributes, ranks, and the detected drawbacks. Accordingly, PM provided sub-optimal illumination with slight brightness amplification in the bright areas. Thus, it scored above high in LOE, BMPRI, CQM, and GM-LOG, but below mediocre in PIQE, while being the 7th fastest in RT, recording an average of 48.9 seconds. The FbM introduced shadows to certain image regions due to the use of the standard CLAHE method. This justifies scoring below high in LOE, lowest in BMPRI, and mediocre in CQM, above high in PIEQ, and low in GM-LOG, while ranking as the 6th fastest in RT, with an average time of 9.8 seconds.

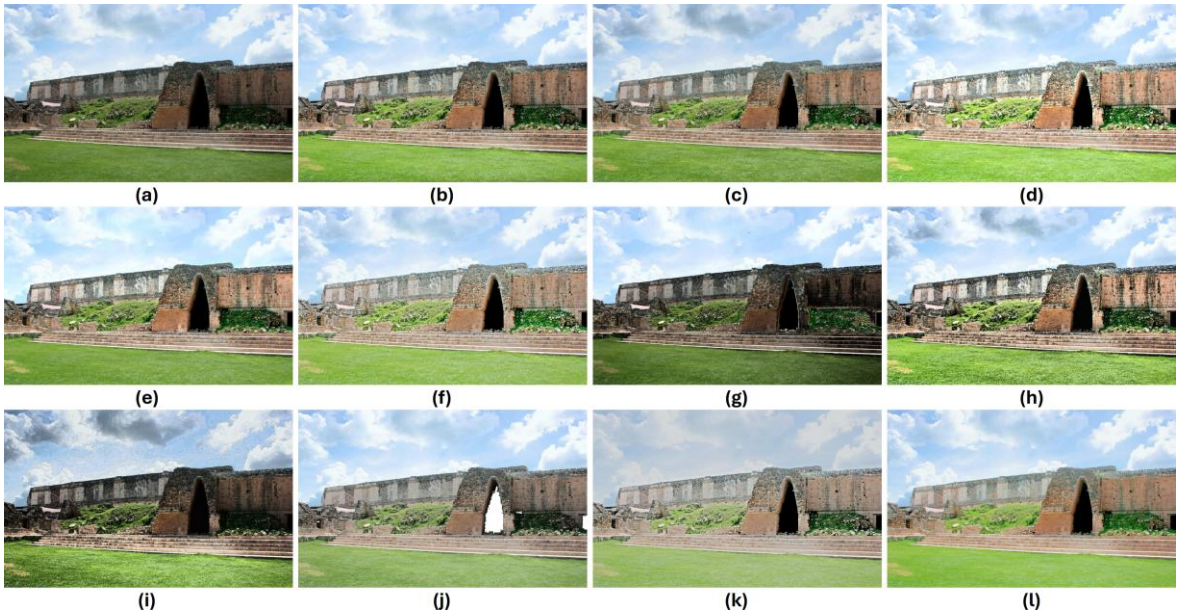

Figure 11. Results of comparisons (Batch 2): (a) Original image; images (b-l) are processed by: (b) PM; (c) FbM; (d) LIME; (e) LightenNet; (f) LECARM; (g) GbM; (h) RM; (i) ShSm; (j) TSM; (k) Retinexformer; (l) Log-Stat.

Figure 12. Results of comparisons (Batch 3): (a) Original image; images (b-l) are processed by: (b) PM; (c) FbM; (d) LIME; (e) LightenNet; (f) LECARM; (g) GbM; (h) RM; (i) ShSm; (j) TSM; (k) Retinexformer; (l) Log-Stat.

LIME, on the other hand, provided unnatural highlights and brightness amplification in certain regions with brightened colors. This is why it attained the lowest in LOE, above mediocre in BMPRI, below high in CQM, low in PIQE, and below mediocre in GM-LOG, with a relatively fast implementation, ranking the 2nd fastest in RT, with an average speed of 5.2 seconds. The LightenNet, on the other hand, introduced a haloing effect around edges and unnatural illumination, especially in dark scenes. This justifies its scoring, low in LOE, below mediocre in BMPRI, above mediocre in CQM, below high in PIQE, and high in GM-LOG. Speaking of RT, it was the slowest comparison method, operating at an average of 188.1 seconds. In contrast, LECARM delivered abnormal illumination in the dark areas, scoring below mediocre in LOE and below low in BMPRI, high in CQM and PIQE, and mediocre in GM-LOG, while averaging at 8.1 seconds in RT, placing 5th rank.

As for GbM, it introduced illumination errors, insufficient illumination, and distortions. This explains the recorded scores above mediocre in LOE and GM-LOG, low in BMPRI, while scoring the lowest in CQM and PIQE, ranking as the 9th slowest algorithm in the comparison. RM produced shadows and distortions due to the use of the standard CLAHE method, which rationalizes the performances of above low in LOE and CQM, mediocre in BMPRI and PIQE, and lowest in GM-LOG, while placing 4th in RT. ShSm also introduced shadows and distortions because of CLAHE utilization, but with varying levels. This justifies ranking mediocre in LOE, high in BMPRI, below low in PIQE, and above low in PIQE and GM-LOG. In terms of RT, it was the 3rd fastest. The TSM generated distortions (Figure 11i) and insufficient illumination. Yet, it scored high in LOE, above low in BMPRI, below mediocre in CQM, above mediocre in PIQE, and below high in GM-LOG, placing 8th rank in RT, averaging 50.8 seconds. Retinexformer provided varying performances as the contrast was deficient, the colors were slightly pale, and the whiteness in the resulting images tended to be yellowish. This explains scoring below low in LOE, below high in BMPRI, low in CQM, and below low in PIQE and GM-LOG. As for RT, this method was the second slowest among the competitors. The proposed Log-Stat algorithm performed the best in all measures. This is a significant advancement as the resulting images by Log-Stat have natural illumination, high perceptual clarity, vivid colors, minimal visual distortions, and are obtained in a few seconds. These qualities are important for accurate archaeological findings, especially when images are captured in uncontrolled or non-ideal lighting conditions. Moreover, Log-Stat achieves this efficiently, processing large images in an average of just 2.4 seconds. This rapid execution makes the method highly practical for real-time or on-site applications. The combination of visual clarity and computational speed underscores the Log-Stat's potential for integration into post-processing workflows and fieldwork.

Figure 13. Results of comparisons (Batch 4): (a) Original image; images (b-l) are processed by: (b) PM; (c) FbM; (d) LIME; (e) LightenNet; (f) LECARM; (g) GbM; (h) RM; (i) ShSm; (j) TSM; (k) Retinexformer; (l) Log-Stat.

Table 1. RT scores ↓ of the comparison.

#	Algorithms	Figure 10	Figure 11	Figure 12	Figure 13	Average	Rank
1	PM	102.824	26.165	27.086	39.589	48.916	7th
2	FbM	21.120	3.548	6.900	7.731	9.824	6th
3	LIME	9.312	2.380	4.537	4.716	5.236	2nd
4	LightenNet	382.751	72.583	135.895	161.308	188.134	11th
5	LECARM	14.285	3.330	6.491	8.373	8.119	5th
6	GbM	148.972	39.516	40.288	38.310	66.771	9th
7	RM	15.047	2.535	5.677	5.766	7.256	4th
8	ShSm	10.867	2.152	4.202	4.826	5.511	3rd
9	TSM	136.140	15.749	46.460	5.212	50.890	8th
10	Retinexformer	308.582	75.814	133.286	61.012	144.673	10th
11	Log-Stat	4.349	1.070	2.0487	2.147	2.403	1st

Table 2. LOE scores ↓ of the comparison.

#	Algorithms	Figure 10	Figure 11	Figure 12	Figure 13	Average	Rank
1	PM	112.653	247.252	194.801	149.699	176.101	2nd
2	FbM	439.646	435.024	348.447	264.396	371.878	4th
3	LIME	1058.800	1280.200	1134.100	475.512	987.153	11th
4	LightenNet	672.504	702.240	1020.300	597.401	748.111	9th
5	LECARM	746.188	741.846	690.645	291.088	617.441	7th
6	GbM	483.855	655.782	359.066	382.355	470.264	5th
7	RM	584.585	708.174	645.666	601.127	634.888	8th
8	ShSm	735.189	572.511	407.902	366.432	520.508	6th
9	TSM	154.698	434.263	169.655	119.474	219.522	3rd
10	Retinexformer	531.314	1419.600	1041.400	367.760	840.018	10th
11	Log-Stat	107.039	204.899	159.521	113.901	146.340	1st

Table 3. BMPRI scores ↑ of the comparison.

#	Algorithms	Figure 10	Figure 11	Figure 12	Figure 13	Average	Rank
1	PM	22.816	19.104	13.248	28.201	20.842	2nd
2	FbM	20.713	10.737	11.374	24.824	16.912	11th
3	LIME	22.646	13.114	11.152	29.217	19.032	5th
4	LightenNet	20.594	10.780	11.003	30.091	18.117	7th
5	LECARM	21.576	11.326	11.161	23.966	17.007	10th
6	GbM	20.578	10.621	15.729	24.492	17.855	9th
7	RM	22.130	15.455	13.075	22.724	18.346	6th
8	ShSm	22.312	17.913	13.486	27.271	20.245	3rd
9	TSM	18.355	12.289	10.823	30.896	18.090	8th
10	Retinexformer	19.401	11.888	18.368	29.043	19.675	4th
11	Log-Stat	23.232	21.210	13.585	28.924	21.737	1st

Table 4. CQM scores ↑ of the comparison.

#	Algorithms	Figure 10	Figure 11	Figure 12	Figure 13	Average	Rank
1	PM	0.138	0.203	0.278	0.115	0.183	2nd
2	FbM	0.139	0.188	0.260	0.107	0.173	6th
3	LIME	0.152	0.199	0.286	0.072	0.177	4th
4	LightenNet	0.133	0.208	0.268	0.092	0.175	5th
5	LECARM	0.156	0.187	0.274	0.104	0.180	3rd
6	GbM	0.086	0.103	0.188	0.042	0.104	11th
7	RM	0.140	0.183	0.245	0.103	0.167	8th
8	ShSm	0.098	0.140	0.177	0.062	0.119	10th
9	TSM	0.146	0.210	0.261	0.064	0.170	7th
10	Retinexformer	0.154	0.157	0.213	0.128	0.163	9th
11	Log-Stat	0.165	0.227	0.276	0.123	0.197	1st

Table 5. PIQE scores ↓ of the comparison.

#	Algorithms	Figure 10	Figure 11	Figure 12	Figure 13	Average	Rank
1	PM	24.318	29.515	14.618	23.095	22.886	7th
2	FbM	18.398	30.415	19.509	10.402	19.681	2nd
3	LIME	21.340	31.495	27.001	12.799	23.158	9th
4	LightenNet	19.449	30.554	21.613	13.258	21.218	4th
5	LECARM	18.728	29.462	21.564	11.450	20.301	3rd
6	GbM	20.874	33.646	26.949	13.164	23.658	11th
7	RM	20.461	33.519	22.114	14.898	22.748	6th
8	ShSm	20.162	35.800	22.861	13.726	23.137	8th
9	TSM	19.717	23.841	19.214	22.715	21.371	5th
10	Retinexformer	18.117	28.735	36.079	9.840	23.192	10th
11	Log-Stat	18.261	26.137	11.530	13.280	17.302	1st

Table 6. GM-LOG scores ↑ of the comparison.

#	Algorithms	Figure 10	Figure 11	Figure 12	Figure 13	Average	Rank
1	PM	8.041	9.067	7.581	5.392	7.520	2nd
2	FbM	6.711	7.657	6.200	4.862	6.357	9th
3	LIME	6.788	8.307	6.555	5.584	6.808	7th
4	LightenNet	7.946	8.985	6.818	6.118	7.466	3rd
5	LECARM	6.635	8.545	6.812	5.278	6.817	6th
6	GbM	6.971	8.592	6.671	5.287	6.880	5th
7	RM	6.539	6.663	5.623	5.223	6.012	11th
8	ShSm	7.319	7.968	6.266	5.004	6.639	8th
9	TSM	7.014	8.201	8.542	5.462	7.304	4th
10	Retinexformer	7.183	8.002	5.569	4.576	6.332	10th
11	Log-Stat	7.029	10.115	8.553	5.675	7.843	1st

Despite the disadvantages, noise still appears when the dark parts are enhanced, because it already exists, and balancing the illumination further reveals such hidden noise. Therefore, a fast and efficient denoising method should be utilized to attain better quality results. Illuminance balancing can significantly contribute to archaeological documentation, analysis, and 3D modeling. In this study, unevenly-illuminated archaeological images were utilized to facilitate qualitative comparisons with recognized benchmarks and to ensure objective evaluations with reproducible conditions. The proposed Log-Stat algorithm was developed with these issues in mind, focusing on robust processing with various illumination conditions. Furthermore, because Log-Stat is based on mathematical transformations rather than on data-driven training, it is inherently generalized and not limited to a definite dataset. Improving details in unevenly-illuminated archaeological photographs can enhance the visibility of petroglyphs, inscriptions, eroded carvings, or other related subjects. Moreover, when creating 3D models from images, illumination irregularities can generate artifacts in the model. Thus, balancing illumination before 3D modeling ensures that textures are constant and more realistic.

5. CONCLUSION

This paper introduces a low-complexity illumination-balancing algorithm that integrates logarithmic approaches with statistical methods to balance the inconsistent illumination and adjust the tonality of archeological images. This combination allowed for better revealing of structural details and important textures. The Log-Stat was tested with various real-world scenes, compared with prominent algorithms, and the outcomes were evaluated using six measures. The products of experiments demonstrated substantial enhancements in illumination and visibility, providing more clarity to the resulting images. Likewise, experiments showed Log-Stat's competence to handle various scenes with different illumination levels. The comparisons also showed Log-Stat favorability in various visual aspects and processing speed. This study is beneficial in the field of digitalization, especially in 3D modeling, analysis, or documentation. For example, if 3D models were created with images having inconsistent illuminations, the model would have dark regions, making it less desirable for usage. Follow-up research can aim for automation *via* perceptual features. This can contribute to making Log-Stat fully automated using a tailored approach.

REFERENCES

[1] C. Morgan and H. Wright, "Pencils and Pixels: Drawing and Digital Media in Archaeological Field Recording," Journal of Field Archaeology, vol. 43, no. 2, pp. 136–151, 2018.

[2] O. A. Basheer and Z. Al-Ameen, "Illumination Enhancement of Nighttime Images Using a Regulated Single Scale Retinex Algorithm," Jordanian Journal of Computers and Information Technology (JJCIT), vol. 10, no. 2, pp. 138–151, 2024.

[3] P. Sapirstein and S. Murray, "Establishing Best Practices for Photogrammetric Recording during Archaeological Fieldwork," Journal of Field Archaeology, vol. 42, no. 4, pp. 337–350, 2017.

[4] H. Kaur and N. Sohi, "A Novel Enhancement Method for Colored Rock Art Archaeological Images," Int. J. Adv. Res. Comput. Sci. (IJARCS), vol. 8, no. 7, pp. 1163–1167, 2017.

[5] S. Sylaiou et al., "Redefining Archaeological Research: Digital Tools, Challenges and Integration in Advancing Methods," Applied Sciences, vol. 15, no. 5, p. 2495, 2025.

[6] L. Marchesotti, N. Murray and F. Perronnin, "Discovering Beautiful Attributes for Aesthetic Image Analysis," Int. J. of Computer Vision (IJCV), vol. 113, pp. 246–266, 2015.

[7] M. G. Robinson, Photogrammetry for Archaeological Objects: A Manual, ISBN-10, 1743329830, Sydney, Australia: Sydney Univ. Press, 2024.

[8] S. Kang et al., "Image Intrinsic Components Guided Conditional Diffusion Model for Low-light Image Enhancement," IEEE Trans. Circuits Syst. Video Technol., vol. 34, no. 12, pp. 13244–13256, 2024.

[9] S. Xu, X. Chen, B. Song, C. Huang and J. Zhou, "CNN Injected Transformer for Image Exposure Correction," Neurocomputing, vol. 587, p. 127688, 2024.

[10] N. Singhal, A. Kadam, P. Kumar, H. Singh and A. Thakur, "Study of Recent Image Restoration Techniques: A Comprehensive Survey," Jordanian Journal of Computers and Information Technology (JJCIT), vol. 11, no. 2, pp. 211–237, 2025.

[11] X. Fu et al., "A Probabilistic Method for Image Enhancement with Simultaneous Illumination and Reflectance Estimation," IEEE Trans. Image Process., vol. 24, no. 12, pp. 4965–4977, 2015.

[12] X. Fu et al., "A Fusion-based Enhancing Method for Weakly Illuminated Images," Signal Process., vol. 129, pp. 82–96, 2016.

[13] X. Guo, Y. Li and H. Ling, "LIME: Low-light Image Enhancement *via* Illumination Map Estimation," IEEE Trans. Image Process., vol. 26, no. 2, pp. 982–993, 2017.

[14] Y. Ren, Z. Ying, T. H. Li and G. Li, "LECARM: Low-light Image Enhancement Using the Camera Response Model," IEEE Trans. Circuits Syst. Video Technol., vol. 29, no. 4, pp. 968–981, 2018.

[15] M. Tanaka, T. Shibata and M. Okutomi, "Gradient-based Low-light Image Enhancement," Proc. of the 2019 IEEE Int. Conf. on Consumer Electronics (ICCE), DOI: 10.1109/ICCE.2019.8662059, Las Vegas, NV, USA, Jan. 2019.

[16] J. Xie et al., "Semantically-guided Low-light Image Enhancement," Pattern Recognition Letters, vol. 138, pp. 308–314, 2020.

[17] N. Singh and A. K. Bhandari, "Principal Component Analysis-based Low-light Image Enhancement Using Reflection Model," IEEE Trans. Instrum. Meas., vol. 70, pp. 1–10, 2021.

[18] J. J. Jeon and I. K. Eom, "Low-light Image Enhancement Using Inverted Image Normalized by Atmospheric Light," Signal Process., vol. 196, p. 108523, 2022.

[19] Y. Demir and N. H. Kaplan, "Low-light Image Enhancement Based on Sharpening-Smoothing Image Filter," Digital Signal Processing, vol. 138, p. 104054, 2023.

[20] M. F. Hassan, T. Adam, H. Rajagopal and R. Paramesran, "A Hue Preserving Uniform Illumination Image Enhancement *via* Triangle Similarity Criterion in HSI Color Space," Visual Computer, vol. 39, no. 12, pp. 6755–6766, 2023.

[21] L. Wang, L. Zhao, T. Zhong and C. Wu, "Low-light Image Enhancement Using Generative Adversarial Networks," Scientific Reports, vol. 14, no. 1, p. 18489, 2024.

[22] I. M. Majid Mohammed and N. A. Mat Isa, "Contrast Limited Adaptive Local Histogram Equalization Method for Poor Contrast Image Enhancement," IEEE Access, vol. 13, pp. 62600–62632, 2025.

[23] S. Yang, D. Zhou, J. Cao and Y. Guo, "LightingNet: An Integrated Learning Method for Low-light Image Enhancement," IEEE Trans. Comput. Imaging, vol. 9, pp. 29–42, 2023.

[24] C. Zhang, K. M. Lam and Q. Wang, "CoF-Net: A Progressive Coarse-to-fine Framework for Object Detection in Remote-sensing Imagery," IEEE Trans. Geosci. Remote Sens., vol. 61, pp. 1–17, 2023.

[25] S. J. Im, C. Yun, S. J. Lee and K. R. Park, "Artificial Intelligence-based Low-light Marine Image Enhancement for Semantic Segmentation in Edge-intelligence-empowered Internet of Things Environment," IEEE Internet Things J., vol. 12, no. 4, pp. 4086–4114, 2025.

[26] C. Li, J. Guo, F. Porikli and Y. Pang, "LightenNet: A Convolutional Neural Network for Weakly Illuminated Image Enhancement," Pattern Recognition Letters, vol. 104, pp. 15–22, 2018.

[27] M. Afifi et al., "CIE XYZ Net: Unprocessing Images for Low-level Computer Vision Tasks," IEEE Trans. Pattern Anal. Mach. Intell., vol. 44, no. 9, pp. 4688–4700, 2022.

[28] Y. Cai, H. Bian, J. Lin, H. Wang, R. Timofte and Y. Zhang, "Retinexformer: One-stage Retinex-based Transformer for Low-light Image Enhancement," Proc. of the IEEE/CVF Int. Conf. on Computer Vision (ICCV), pp. 12504–12513, 2023.

[29] Y. Cui, W. Ren, X. Cao and A. Knoll, "Revitalizing Convolutional Network for Image Restoration," IEEE Trans. Pattern Anal. Mach. Intell., vol. 46, no. 12, pp. 9423–9438, 2024.

[30] L. Xu, C. Hu, Y. Hu, X. Jing, Z. Cai and X. Lu, "UPT-Flow: Multi-scale Transformer-guided Normalizing Flow for Low-light Image Enhancement," Pattern Recognition, vol. 158, p. 111076, 2025.

[31] S. Bansal, R. K. Bansal and R. Bhardwaj, "A Novel Low Complexity Retinex-based Algorithm for Enhancing Low-light images," Multimedia Tools Appl., vol. 83, no. 10, pp. 29485–29504, 2024.

[32] A. Łoza et al., "Automatic Contrast Enhancement of Low-light Images Based on Local Statistics of Wavelet Coefficients," Digital Signal Processing, vol. 23, no. 6, pp. 1856–1866, 2013.

[33] M. Jourlin and J. C. Pinoli, "A Model for Logarithmic Image Processing," Journal of Microscopy, vol. 149, no. 1, pp. 21–35, 1988.

[34] X. Pei et al., "Robustness of Machine Learning to Color, Size Change, Normalization and Image Enhancement on Micrograph Datasets with Large Sample Differences," Materials & Design, vol. 232, p. 112086, 2023.

[35] O. Bryan et al., "A Diffusion-based Super Resolution Model for Enhancing Sonar Images," Journal of the Acoustical Society of America, vol. 157, no. 1, pp. 509–518, 2025.

[36] M. Ambrosanio, B. Kanoun and F. Baselice, "WKSR-NLM: An Ultrasound Despeckling Filter Based on Patch Ratio and Statistical Similarity," IEEE Access, vol. 8, pp. 150773–150783, 2020.
[37] S. Wang, J. Zheng, H. M. Hu and B. Li, "Naturalness Preserved Enhancement Algorithm for Non-uniform Illumination images," IEEE Trans. Image Process., vol. 22, no. 9, pp. 3538–3548, 2013.
[38] X. Min, G. Zhai, K. Gu, Y. Liu and X. Yang, "Blind Image Quality Estimation *via* Distortion Aggravation," IEEE Trans. on Broadcasting, vol. 64, no. 2, pp. 508–517, 2018.
[39] C. Gao, K. Panetta and S. Agaian, "Color Image Attribute and Quality Measurements," Proc. SPIE Mobile Multimedia/Image Processing, Security and Applications, vol. 9120, pp. 238–251, May 2014.
[40] N. Venkatanath, D. Praneeth, S. C. Sumohana and S. M. Swarup, "Blind Image Quality Evaluation Using Perception-based Features," Proc. of the 2015 21st National Conf. on Communications (NCC), pp. 1–6, Mumbai, India, 2015.
[41] W. Xue et al., "Blind Image Quality Assessment Using Joint Statistics of Gradient Magnitude and Laplacian Features," IEEE Trans. Image Process., vol. 23, no. 11, pp. 4850–4862, 2014.
[42] N. Singh and A. K. Bhandari, "Noise Aware L_2–LP Decomposition-based Enhancement in Extremely Low Light Conditions with Web Application," IEEE Trans. on Consumer Electronics, vol. 68, no. 2, pp. 161–169, 2022.

ملخص البحث:

في بعض الأحيان، يتمّ التقاط الصُّور الأثرية في بيئات تتّسم بإضاءةٍ غير مثالية، الأمر الّذي يؤدّي إلى إضاءةٍ غير متوازنة وفقدان بعض التّفاصيل. وتعملُ مثل هذه المشكلات على إعاقة بعض العمليات، مثل التّحليل والتّفسير والتّمثيل والنّمذجة ثلاثية الأبعاد.

تُقدّم هذه الدّراسة خوارزميةً من شأنها أن تعمل على تحقيق توازن الإضاءة، وهي خوارزمية لوغاريتمية-إحصائية تحمِلُ اسم "Log-Stat"، وتتكوّن من مرحلتين: الأولى تَستخدم ستَّ عملياتٍ رياضية، بينما تستفيد الثانية من أربعِ عملياتٍ.

تمّ استخدامُ صُور متنوّعة لفحص الخوارزمية، وجرت مقارنة الخوارزمية المقترحة مع عَشر خوارزميات مشهورة، وذلك باستخدام ستّة مؤشّرات أداءٍ. وقدْ برهنت المقارنة على نجاح الخوارزمية المقترحة في عددٍ من الجوانب المختلفة، منها استعادة الوضوح وتحقيقُ توازن الإضاءة، الأمر الّذي يؤدّي إلى دقّة في التّفاصيل الّتي يمكن أن تتأثّر سلباً بغياب توازن الإضاءة في الصُّور الأصلية. والجدير بالذّكر أنّ ذلك يؤكّد نجاعة الخوارزمية المقترحة في هذه الدّراسة في تحسين جودة الصُّور الأثرية الملتقطة في ظروف إضاءةٍ غير مثالية.